Disruption of the Vacuolar Calcium-ATPases in Arabidopsis Results in the Activation of a Salicylic Acid-Dependent Programmed Cell Death Pathway[1][W][OA]

Yann Boursiac[2,3], Sang Min Lee[2], Shawn Romanowsky, Robert Blank, Chris Sladek, Woo Sik Chung, and Jeffrey F. Harper*

Biochemistry Department (Y.B., S.R., C.S., J.F.H.) and United States Department of Agriculture (R.B.), University of Nevada, Reno, Nevada 89557; and Division of Applied Life Science (BK21 Program), Plant Molecular Biology and Biotechnology Research Center, Gyeongsang National University, 900 Gajwa, Jinju, Korea (S.M.L., W.S.C.)

Calcium (Ca^{2+}) signals regulate many aspects of plant development, including a programmed cell death pathway that protects plants from pathogens (hypersensitive response). Cytosolic Ca^{2+} signals result from a combined action of Ca^{2+} influx through channels and Ca^{2+} efflux through pumps and cotransporters. Plants utilize calmodulin-activated Ca^{2+} pumps (autoinhibited Ca^{2+}-ATPase [ACA]) at the plasma membrane, endoplasmic reticulum, and vacuole. Here, we show that a double knockout mutation of the vacuolar Ca^{2+} pumps ACA4 and ACA11 in Arabidopsis (*Arabidopsis thaliana*) results in a high frequency of hypersensitive response-like lesions. The appearance of macrolesions could be suppressed by growing plants with increased levels (greater than 15 mM) of various anions, providing a method for conditional suppression. By removing plants from a conditional suppression, lesion initials were found to originate primarily in leaf mesophyll cells, as detected by aniline blue staining. Initiation and spread of lesions could also be suppressed by disrupting the production or accumulation of salicylic acid (SA), as shown by combining *aca4/11* mutations with a *sid2* (for *salicylic acid induction-deficient2*) mutation or expression of the SA degradation enzyme NahG. This indicates that the loss of the vacuolar Ca^{2+} pumps by itself does not cause a catastrophic defect in ion homeostasis but rather potentiates the activation of a SA-dependent programmed cell death pathway. Together, these results provide evidence linking the activity of the vacuolar Ca^{2+} pumps to the control of a SA-dependent programmed cell death pathway in plants.

Calcium (Ca^{2+}) signals have been implicated in regulating many aspects of plant growth and responses to the environment (for recent summaries, see McAinsh and Pittman, 2009; Dodd et al., 2010; Kudla et al., 2010). Some of the most well-studied examples include regulation of guard cells and transpiration (Israelsson et al., 2006; Pandey et al., 2007; Neill et al., 2008; Sirichandra et al., 2009), symbiosis and nodulation in legumes (Oldroyd and Downie, 2004; Kosuta et al., 2008), polarized growth (Bosch and Franklin-Tong, 2008; Bothwell et al., 2008), pathogen response (Lecourieux et al., 2006; Ma et al., 2008; Moeder and Yoshioka, 2008), and salt stress (Mahajan et al., 2008; Qudeimat et al., 2008; Song et al., 2008). Additionally, in both plants and animals, cytosolic Ca^{2+} signals have been linked to the activation of programmed cell death (PCD; Lecourieux et al., 2006; Clapham, 2007; Ma and Berkowitz, 2007; Verkhratsky, 2007; Bosch and Franklin-Tong, 2008; Moeder and Yoshioka, 2008; Reape et al., 2008; Lee and McNellis, 2009; Zhu et al., 2010).

A cytoplasmic Ca^{2+} signal is shaped by the balance of activity between Ca^{2+} influx and efflux. Influx occurs down an electrochemical gradient through various ion channels, such as Ca^{2+}-permeable cyclic nucleotide-gated channels (CNGCs) or voltage-gated channels such as two-pore channel (TPC; Pottosin and Schönknecht, 2007; McAinsh and Pittman, 2009; Ward et al., 2009). Ca^{2+} can enter the cytoplasm from several sources, including the apoplast, endoplasmic reticulum (ER), vacuole, chloroplast, or mitochondria. Efflux

[1] This work was supported by grants to J.F.H. from the National Science Foundation (grant no. DBI–0077378 for ionomics and no. DBI–0420033 for phenotype studies) and the National Institutes of Health (grant no. 1RO1 GM070813–01 for genetic analyses and no. DE–FG03–94ER20152 for studies on the vacuolar regulation of programmed cell death). Mass spectrometry and bioinformatics were made possible by the IDeA Network of Biomedical Research Excellence Program of the National Center for Research Resources (National Institutes of Health grant no. P20 RR–016464). W.S.C. was supported by the World Class University Program (grant no. R32–10148) funded by the Ministry of Education, Science and Technology and by the BioGreen 21 Program (grant no. 20080401034023) funded by the Rural Development Administration.

[2] These authors contributed equally to the article.

[3] Present address: Biochemistry and Plant Molecular Physiology, UMR5004, 34060 Montpellier, France.

* Corresponding author; e-mail jfharper@unr.edu.

The author responsible for distribution of materials integral to the findings presented in this article in accordance with the policy described in the Instructions for Authors (www.plantphysiol.org) is: Jeffrey F. Harper (jfharper@unr.edu).

[W] The online version of this article contains Web-only data.

[OA] Open Access articles can be viewed online without a subscription.

www.plantphysiol.org/cgi/doi/10.1104/pp.110.159038

requires energy-dependent Ca^{2+} pumps (autoinhibited Ca^{2+}-ATPases [ACAs] and ER-type Ca^{2+}-ATPases) or cotransport systems, such as Ca^{2+}/proton exchangers (CAXs; McAinsh and Pittman, 2009). As with channels, different efflux systems are present in different membrane systems, each with various regulatory controls. The different subcellular locations of these Ca^{2+} circuits may contribute to the unique information content of different Ca^{2+} signals and help provide a mechanism for creating stimulus-specific Ca^{2+} signatures.

Plants appear to have three groups of ACAs, located in the plasma membrane, ER, and tonoplast (vacuolar membrane; Baxter et al., 2003). In Arabidopsis (*Arabidopsis thaliana*), the vacuoles are equipped with both CAXs (McAinsh and Pittman, 2009) and two closely related ACAs, isoforms ACA4 and ACA11 (Geisler et al., 2000; Lee et al., 2007). While both transport systems are regulated by autoinhibitors, the activation signals for CAXs remain to be determined (McAinsh and Pittman, 2009). However, ACAs are known to be stimulated by Ca^{2+}/calmodulin, providing a direct feedback pathway for a Ca^{2+} signal to turn itself off. Arabidopsis has eight additional ACAs, three of which are thought to be located in the ER and five in the plasma membrane (Baxter et al., 2003; Boursiac and Harper, 2007). The activity of an ER-located ACA has been shown to be inhibited through phosphorylation by a Ca^{2+}-dependent protein kinase (Hwang et al., 2000). This provides a precedent that the activity of some ACAs can be modulated by two different Ca^{2+} signaling pathways, one that activates and the other that inhibits. Altering the balance between these two pathways may provide a mechanism to finely regulate a stimulus-specific Ca^{2+} signature.

In animal cells, genetic disruptions of Ca^{2+} pumps have resulted in multiple phenotypes, including lethality, deafness, muscle and skin disorders, increased frequency of cancer (Okunade et al., 2007; Song et al., 2008), and male sterility and apoptosis (Okunade et al., 2004, 2007; Prasad et al., 2007; Vafiadaki et al., 2009). In Arabidopsis, disruptions of ER-type Ca^{2+}-ATPases have revealed defects in vegetative development and Mn^{2+} homeostasis, while disruptions of ACAs have been linked to defects in pollen tube growth, sperm cell discharge, and cell elongation in vegetative development (Wu et al., 2002; Schiøtt et al., 2004; George et al., 2008; Li et al., 2008).

Evidence that ACAs can modulate biotic and abiotic stress response pathways has recently been obtained from experiments with moss and tobacco (*Nicotiana tabacum*). In the moss *Physcomitrella patens*, a knockout of a gene encoding the vacuolar ACA (*PCA1*) resulted in an increased sensitivity to NaCl stress, which was correlated with a NaCl-triggered cytosolic Ca^{2+} elevation that was higher in magnitude and longer in duration (Qudeimat et al., 2008). In tobacco, RNA interference (RNAi) silencing of *NbCA1* resulted in an accelerated pathogen-triggered PCD response (Zhu et al., 2010). An ER location for NbCA1 was proposed based on transient expression of a GFP-tagged pump. The *NbCA1*-RNAi plants also showed elicitor-triggered Ca^{2+} signals that were higher in magnitude and longer in duration. These two examples confirm that ACAs can function to modulate the dynamics of Ca^{2+} signals triggered by multiple environmental signals, as expected for a Ca^{2+}/calmodulin-activated Ca^{2+} pump.

Here, we show that a double disruption of Arabidopsis vacuolar pumps ACA4 and ACA11 results in a high frequency of apoptosis-like lesions. These lesions result from a PCD pathway that is dependent on salicylic acid (SA), similar to PCD pathways associated with a pathogen-triggered hypersensitive response (HR) or various lesion-mimic mutants (Kurusu et al., 2005; Lecourieux et al., 2006; Ma and Berkowitz, 2007; Gadjev et al., 2008; Ma et al., 2008; Moeder and Yoshioka, 2008; Reape et al., 2008). A role for Ca^{2+} signals in many PCD pathways has been well established in both animal systems (Clapham, 2007) and plant systems (Kurusu et al., 2005; Lecourieux et al., 2006; Ma and Berkowitz, 2007; Ma et al., 2008; Moeder and Yoshioka, 2008; Lee and McNellis, 2009; Zhu et al., 2010). However, in plants, the genetic identification of Ca^{2+} transport systems involved in PCD has been limited to mutations associated with Ca^{2+}-permeable ion channels thought to be associated with the plasma membrane (e.g. CNGC or Glu receptors [Lecourieux et al., 2006; Ma and Berkowitz, 2007]) and an RNAi silencing of a proposed ER-located Ca^{2+} pump in tobacco (Zhu et al., 2010). Thus, the identification here of *ACA4* and *ACA11* as genetic suppressors of a PCD pathway establishes a link between vacuole-modulated Ca^{2+} signals and a PCD pathway in plants. This represents a plant-specific variation on the regulation of PCD, as the large central vacuole in plant cells is a feature not found in typical animal cells.

RESULTS

aca4/11 Double Mutants Exhibit HR-Like Lesions in Leaves

To evaluate the biological functions of ACA4 and ACA11 in Arabidopsis, we created two independent sets of double mutants. Two T-DNA insertion mutants in the Wassilewskija (Ws) ecotype (*aca4-1* and *aca11-1*) were isolated from the Arabidopsis Knockout Collection at the University of Wisconsin-Madison (Sussman et al., 2000). Two additional alleles in the Columbia (Col) ecotype were obtained from the Salk Collection (*aca4-3* [SALK_029620.50.70.x]; Alonso et al., 2003) and the Syngenta/Sail Collection (*aca11-5* [269_C07.b.1a.Lb3Fa]; McElver et al., 2001). T-DNA borders for each insertion were PCR amplified, and the exact site of insertion was reconfirmed by DNA sequencing (positions of the left border are shown in Fig. 1). The T-DNA insertions in *aca4-3* and *aca11-1* contain a Basta resistance marker, whereas *aca4-1* and *aca11-5* contain a kanamycin resistance gene.

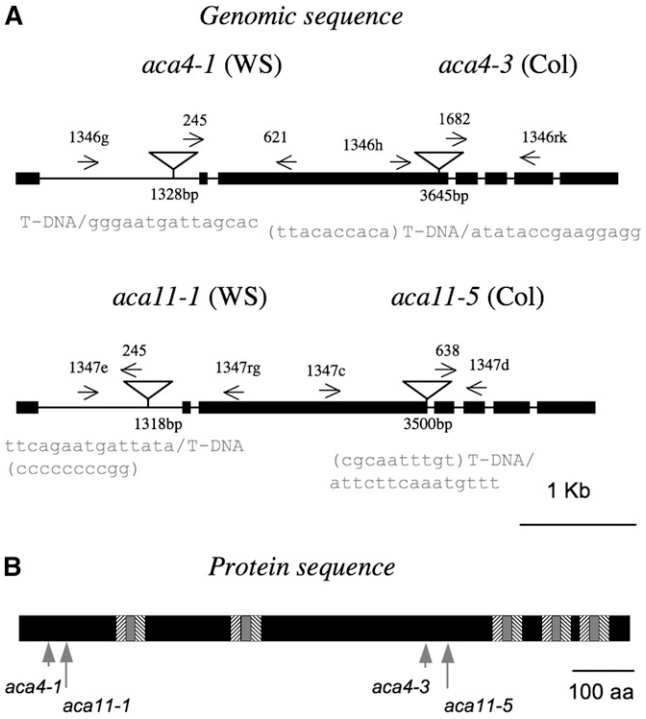

Figure 1. Identification of two independent knockout lines each for *AtACA4* and *AtACA11*. A, Location and direction of the T-DNA insertions on the genomic sequence for the alleles *aca4-1*, *aca4-3*, *aca11-1*, and *aca11-5*. Alleles *4-1* and *11-1* are in the Ws ecotype, and alleles *4-3* and *11-5* are in the Col ecotype. Exons (bars) and introns (lines) are presented according to gene models at the TAIR8 Web site (http://www.arabidopsis.org) for At2g41560 (*ACA4*) and At3g57330 (*ACA11*). The primers corresponding to the T-DNA left border are 245 (5′-CATTTTATAATAACGCTGCGGACATCTAC-3′), 1682 (5′-ATTTGCCGATTTCGGAAC-3′), and 638 (5′-AGGTGAAACTAAATGGTGTTG-3′). Primers used to genotype the alleles are as follows: 1346rk (5′-CCCATCTAGCCACATTTACTATTGTTTTGAAGT-3′), 1346h (5′-GAGGGAAGTAAAGAAAGCTTTGAGTTGGAA-3′), 1347d (5′-ACGTCCCCATTTTGCCACAT-3′), 1347c (5′-GCCTTTTCAGAAATGGATAAATAGCCTTGCTTCC-3′), 621 (5′-AGTAACCATGACCACCAAGAG-3′), 1346g (5′-TCTAATCCACACTTTTGCATAC-3′), 1347rg (5′-CTTCTCTGTTTTGGTCTTTCTTTTTCTTTC-3′), and 1347e (5′-CATTTTATAATAACGCTGCGGACATCTA-3′). B, Location of insertions in the context of the protein topology. Both ACA4 and ACA11 are highly similar and have the same general topology. Gray arrows indicate the sites at which T-DNA insertions would be expected to create truncated transcripts and proteins. The positions of cytosolic and vacuolar loops (black and gray bars, respectively) and transmembrane segments (white bars with stripes) are shown. aa, Amino acids.

While the T-DNA insertion sites for the two Ws alleles are located in the first intron (and therefore are potentially spliced out at some low frequency), the insertion sites for the two Col background alleles, *aca4-3* and *aca11-5*, are located in the coding sequence and are expected to result in truncations or deletions that would disrupt the translation of a functional pump (Fig. 1B). Nevertheless, both sets of double mutants showed a very similar lesion-mimic phenotype (see below). This phenotype was shown to be rescued by the expression of an ACA11 transgene (see below), indicating that the *aca4* and *aca11* double mutations result in a loss of function of vacuolar Ca^{2+} pumping activity.

When grown either hydroponically or in soil, single mutants did not display any strong phenotype. On rare occasions, *aca4-3* exhibited faint chlorotic spots in leaves (data not shown). In contrast, when the double mutants *aca4-1/11-1* (ecotype Ws) and *aca4-3/11-5* (ecotype Col) were grown in soil or hydroponically (with commonly used nutrient concentrations), they both developed HR-like necrotic lesions on leaves, normally within a few days after transfer from germination plates (Fig. 2A). Those lesions appeared as spots that eventually extended to the whole leaf and rosette. At the time of bolting, mutant plants were significantly smaller than wild-type controls (Fig. 2B), most likely due to the cumulative effects of lesions on the plant's photosynthetic productivity. Nevertheless, *aca4/11* plants can complete their life cycle with no apparent defects in reproductive development. Seeds from double mutant plants showed no detectable alteration in germination rates (data not shown).

ACA11-GFP Rescues the *aca4/11* Lesion Phenotype

To confirm that the lesion phenotype was due to the absence of ACA4 and ACA11 Ca^{2+} pumps, the *aca4-3/11-5* double mutant was transformed with a construct encoding ACA11-GFP under the control of either the natural *ACA11* promoter or the *35S* promoter from *Cauliflower mosaic virus*. This ACA11-GFP was previously shown to be targeted to the vacuolar membrane (Lee et al., 2007). Both constructs provided a complete rescue of the lesion phenotype (Fig. 2B). Expression of the expected 137-kD protein was confirmed by a western blot of each rescued line (Fig. 2C).

Anion Supplements Can Suppress the *aca4/11* Lesion Phenotype

Since young plants often showed no lesions while growing on half-strength Murashige and Skoog medium, we tested whether some component of this growth medium could function to suppress lesion formation. To do this, plants were cultivated in hydroponic solutions with varying concentrations of KNO_3, NH_4NO_3, KCl, or KH_2PO_4 (Fig. 3). We observed a suppression of lesion formation for *aca4-1/11-1* (Fig. 3) when our standard hydroponic medium was supplemented with an additional 15 mM NO_3^- in the form of 15 mM KNO_3 or NH_4NO_3 (final $[NO_3^-]$ = 19.25 mM), 15 mM KH_2PO_4 (final $[PO_4^-]$ = 15.5 mM), or 15 mM KCl (final $[Cl^-]$ = 15 mM). While strong suppression was observed with a 15 mM NH_4NO_3 supplement, the identical concentration of ammonium succinate actually led to an increase in the rate of lesion induction (data not shown). Thus, for suppression by NH_4NO_3, it appears that the NO_3^- alone carries the functional suppressor activity. Since there is not a common ion in all three nutrient suppressors (KCl, NH_4NO_3, and

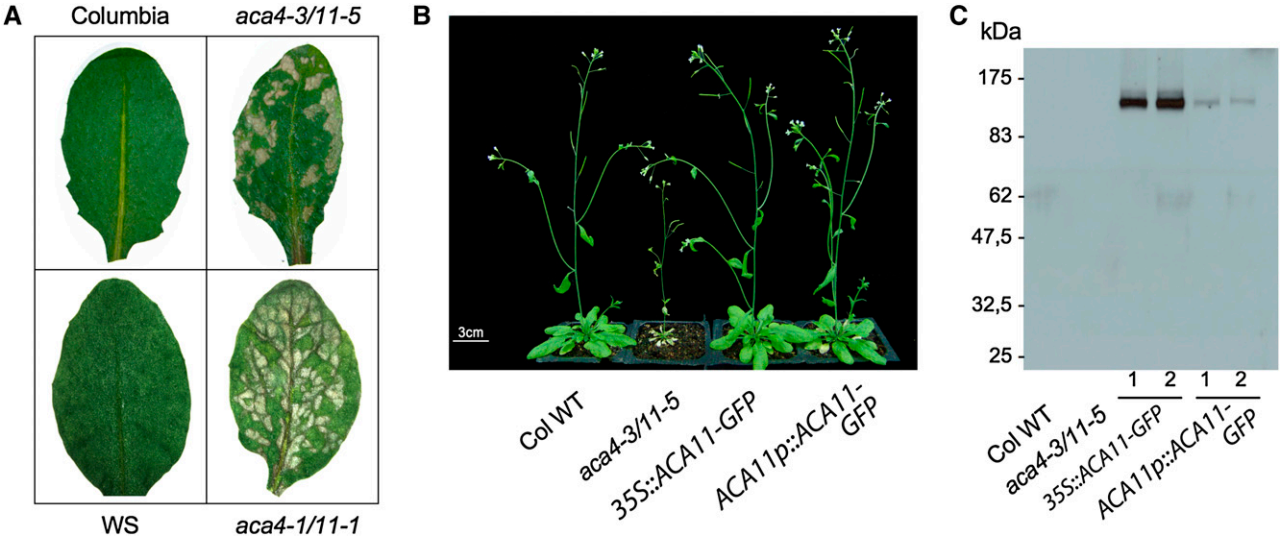

Figure 2. Lesion phenotype in *aca4/11* can be suppressed by transgene expression of an ACA11-GFP fusion. A, Lesions are shown for 20-d-old leaves from plants cultivated hydroponically. Representative images are shown for knockouts and controls in the Col (top panels) and Ws (bottom panels) ecotypes. B, Photograph of soil-grown plants. Col wild-type (WT), *aca4-3/11-5*, and *aca4-3/11-5* plants transformed by the ACA11-GFP construct under the control of the 35S promoter (*35S-ACA11-GFP*) or the native promoter (*ACA11p-ACA11-GFP*) are compared. Rescued lines were recovered at a frequency of 21 out of 28 for the *35S-ACA11-GFP* construct (e.g. seed stock 1355–1358) and two out of eight for the *ACA11p-ACA11-GFP* construct (ss1353 and 1354). C, Immunodetection of the ACA11-GFP fusion. Membrane proteins (30 μg) from wild-type, *aca4-3/11-5*, and two lines of *aca4-3/11-5* plants transformed by the ACA11-GFP construct under the control of the 35S promoter (*35S-ACA11-GFP*) or the native promoter (*ACA11p-ACA11-GFP*) were analyzed by immunoblot for their reaction with an antibody raised against GFP. Bands corresponding to the expected size of the GFP-tagged ACA11 were detected at 137 kD.

KH_2PO_4), and since the NH_4NO_3/NH_4-succinate experiment indicates that NO_3^- alone can function to suppress lesions, these results suggest that the elevated mineral anion component of these nutritional supplements is the functional feature of the nutritional suppression.

While a nutritional suppression was observed for both sets of double knockouts (Col and Ws backgrounds), the conditional suppression in *aca4-3/11-5* (Col background) broke down just after plants initiated a floral bolt. This difference between ecotypes indicates that the observed nutritional suppression can vary as a function of genetic modifiers, some of which might regulate physiological changes that occur during flowering.

Chronology of Lesion Induction

The conditional suppression allowed us to monitor the induction of lesions following a change in nutrient supply. After germination, *aca4-1/11-1* plants were grown without lesions in our standard hydroponic solution supplemented with an additional 15 mM NH_4NO_3. Lesions were then triggered by transferring plants to standard unsupplemented hydroponic solution. Early lesion formation was then monitored during the following 54 to 72 h with diaminobenzidine staining for the detection of reactive oxygen species (ROS) and by aniline blue staining for callose deposition, a standard marker for HR lesions (Dietrich et al., 1994; Figs. 4 and 5; Supplemental Fig. S1).

In controls, wild-type plants before and after transfer from anion-supplemented conditions showed the same low frequency of microlesions (callose staining) and low background levels of ROS (Fig. 4). By contrast, *aca4/11* plants even before transfer showed patches of elevated levels of ROS (Fig. 4A, 0 h; Supplemental Fig. S1) as well as a detectably higher frequency of microlesions (Fig. 4B). This indicates that while the anion supplement prevented any macrolesion expansion, it only partially inhibited lesion initiation. However, by 54 h after transfer from suppression conditions, the surface area covered by patches of ROS had increased more than 2-fold (Fig. 4A). In addition, the number of lesions increased 2.5-fold (Fig. 4B), with a typical lesion increasing in surface area by more than 4-fold from 48 to 72 h (Fig. 4C). In most cases, lesions grew to occupy the entire leaf surface within 3 to 4 d. Thus, this analysis indicates that a period between 30 and 54 h after transfer from lesion suppression conditions provides the earliest time at which a transition from microlesion to macrolesion formation can be visualized.

To identify the cell types in which lesions originate, we mapped the locations of single-cell-sized callose deposits (microlesions) during a 72-h lesion induction experiment (Fig. 5; Supplemental Fig. S2). Under nutritionally suppressed conditions, the microlesions

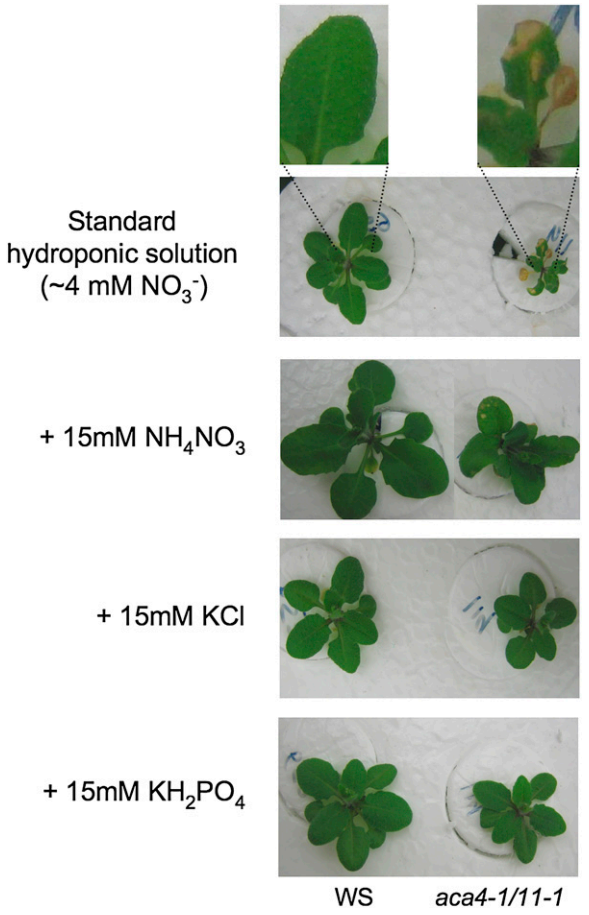

Figure 3. Nutritional supplements suppress the lesion phenotype of *aca4/11*. Nine-day-old seedlings were transferred from in vitro culture to a standard hydroponic solution supplemented with an additional 15 mM NH_4NO_3, 15 mM KCl, or 15 mM KH_2PO_4. Photographs taken 7 d later show the development of lesions in *aca4-1/11-1* plants under standard conditions but not in plants with anion supplements.

detected in *aca4/11* appeared evenly distributed among the internal tissues of the leaf (parenchyma, mesophyll, and vessels), whereas none were observed at the epidermis (Figs. 4B, 0 h, and 5). Within 40 h after transfer to lesion-permissive conditions, the number of microlesions increased, primarily in locations corresponding to mesophyll cells. In a distribution analysis of 117 lesions, 85 microlesions were classified as of mesophyll origin, 25 as parenchyma, and only seven as epidermal. However, since this staining assay was destructive, it did not allow us to observe individual microlesions as they developed into macrolesions. Nevertheless, this distribution analysis provides strong evidence that lesions in *aca4/11* preferentially initiate in mesophyll cells.

Within the group of lesion-mimic mutants, some such as *vad1* (Lorrain et al., 2004) show a high frequency of lesions near the vasculature. This "vascular" pattern may result from the spread of a lesion-triggering signal through the vasculature. To test for this in *aca4/11*, the distribution of lesion initials was evaluated relative to vessels. A lesion was considered vessel associated if was directly adjacent to or within one cell layer (approximately 25 μm). Between 18 and 30 h after lesion

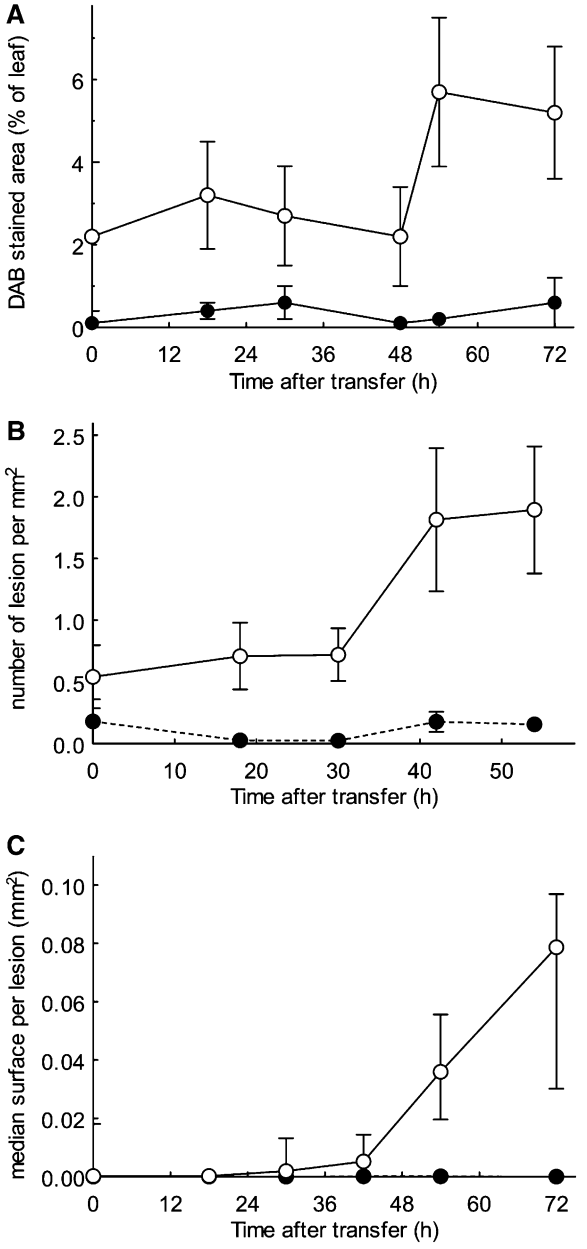

Figure 4. ROS production and callose deposition increase rapidly following the removal of lesion suppression medium. Plants (the wild type in black circles and *aca4/11* in white circles) were grown for 10 d under "suppressing conditions" provided by a 15 mM NH_4NO_3 supplement to the standard hydroponic solution. Plants were then transferred to the standard hydroponic solution for the indicated times before harvest. A, ROS production was monitored by staining with diaminobenzidine (DAB). B, Callose deposition was monitored by staining with aniline blue. C, The area of lesions was calculated from aniline blue-stained leaves. Values and error bars represent means ± SE for A and B and median ± 75th percentile for C. $n = 8$ individual leaves (except for 0 h, for which $n = 4$).

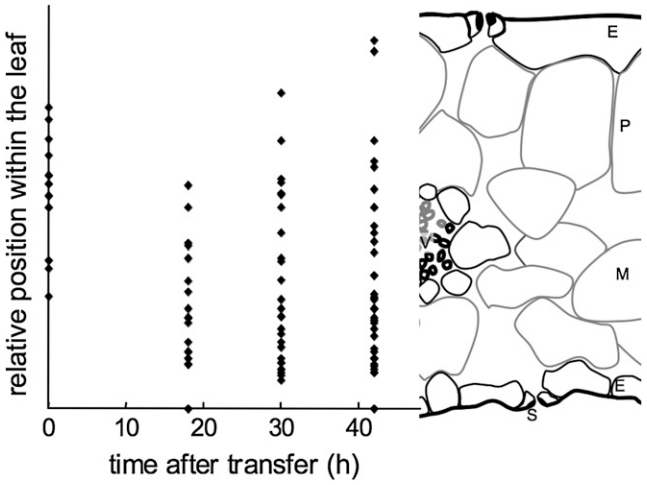

Figure 5. Lesion initials occur preferentially in mesophyll cells, as detected by aniline blue staining. Plants were grown and lesions were induced as explained in Figure 4. Each microlesion was detected as a callose deposit and recorded according to its relative position on the leaf. The diagram to the right shows a transverse cut of an Arabidopsis leaf with labels corresponding to different cell types (E, epidermis; M, mesophyll cells; P, parenchyma cells; S, stomate).

induction, only 12% of the initials were located in the vicinity of a vessel (Supplemental Fig. S3). This suggests that microlesions initiate independently from a potential signal spreading through the vascular system. Together, these lesion-mapping studies suggest that lesion initials arise predominantly in mesophyll cells due to a stimulus that is intrinsic to the region surrounding the initial.

Ca^{2+} Levels in *aca4/11* Plants Are Similar to Wild-Type Levels

To determine if a loss of vacuolar Ca^{2+} pumps would affect the total accumulation of Ca^{2+} (or other ions) in the leaves, we analyzed mutant and wild-type leaves for differences in calcium, iron, potassium, magnesium, manganese, sodium, phosphorus, and sulfur (Fig. 6; Supplemental Fig. S4). Plants were cultivated hydroponically under conditions of nutritional suppression (i.e. with an addition of 15 mM NO_3^-), and the rosettes of both wild-type and *aca4/11* plants were harvested before or 30 h after transfer into a standard hydroponic solution (lesion-permissive condition). Samples were analyzed for levels of mineral nutrients by inductively coupled plasma atomic emission spectroscopy (ICP-AES). Of the cations tested, only potassium showed a potentially significant difference between mutant and wild-type controls, with potassium levels in the *aca4/11* mutant approximately 20% less. While a transfer to lesion-permissive conditions resulted in an approximately 20% increase in potassium levels, the relative difference between the mutant and a wild-type control was not altered (Supplemental Fig. S4).

For total Ca^{2+} levels, there were no significant differences between the wild type and *aca4/11*, although both sets of plants showed a 25% increase in Ca^{2+} when transferred from nutrient-suppressed to lesion-permissive conditions. Therefore, our results indicate that ACA4 and ACA11 are not required for leaves to achieve normal Ca^{2+} storage levels. This is consistent with the hypothesis that CAXs rather than Ca^{2+} pumps have a primary role in Ca^{2+} loading into plant vacuoles (Hirschi, 1999; Kim et al., 2006).

Cl^- and NO_3^- Levels Decrease More Rapidly in *aca4/11* When Switched to Lesion-Triggering Conditions

The relative concentrations were also determined for each of the three anions used here to suppress *aca4/11* lesions (Fig. 7). In plants grown using a 15 mM KCl supplement for lesion suppression (Fig. 7, left panels), chloride content in leaves of both wild-type and *aca4-1/11-1* plants were elevated nearly 10-fold compared with plants grown with a standard hydroponic solution. This elevated level was maintained in wild-type plants during the first 30 h after transfer to our standard hydroponic conditions. In contrast, the mutants showed a 32% loss of Cl^- during this same period.

A similar pattern of anion loss by the mutant was observed for plants transferred from a condition of nutrient suppression using a 15 mM NH_4NO_3 supplement (Fig. 7, middle panels). When plants were transferred from supplemented to standard hydroponic solution, only the mutant showed a relatively rapid decrease (22%) in NO_3^- during this first 30-h period.

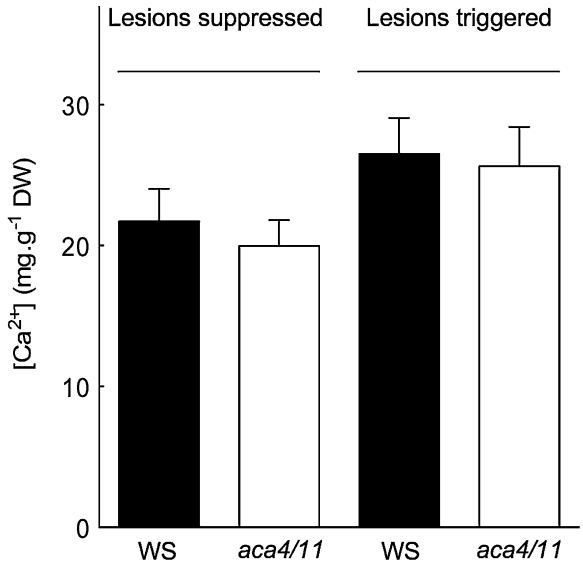

Figure 6. The *aca4-1/11-1* mutants have total Ca^{2+} levels that are similar to the wild type (Ws) under both suppressed and lesion-triggered conditions. Plants were grown hydroponically for 20 d under lesion-suppressed conditions (i.e. with 15 mM NH_4NO_3 supplement) and either harvested directly (lesion-suppressed samples) or transferred to standard hydroponic solution for an additional 30 h before harvest (lesion-triggered samples). Ca^{2+} concentrations were determined by ICP-AES (n = 12 plants) and are reported as means ± SE. DW, Dry weight.

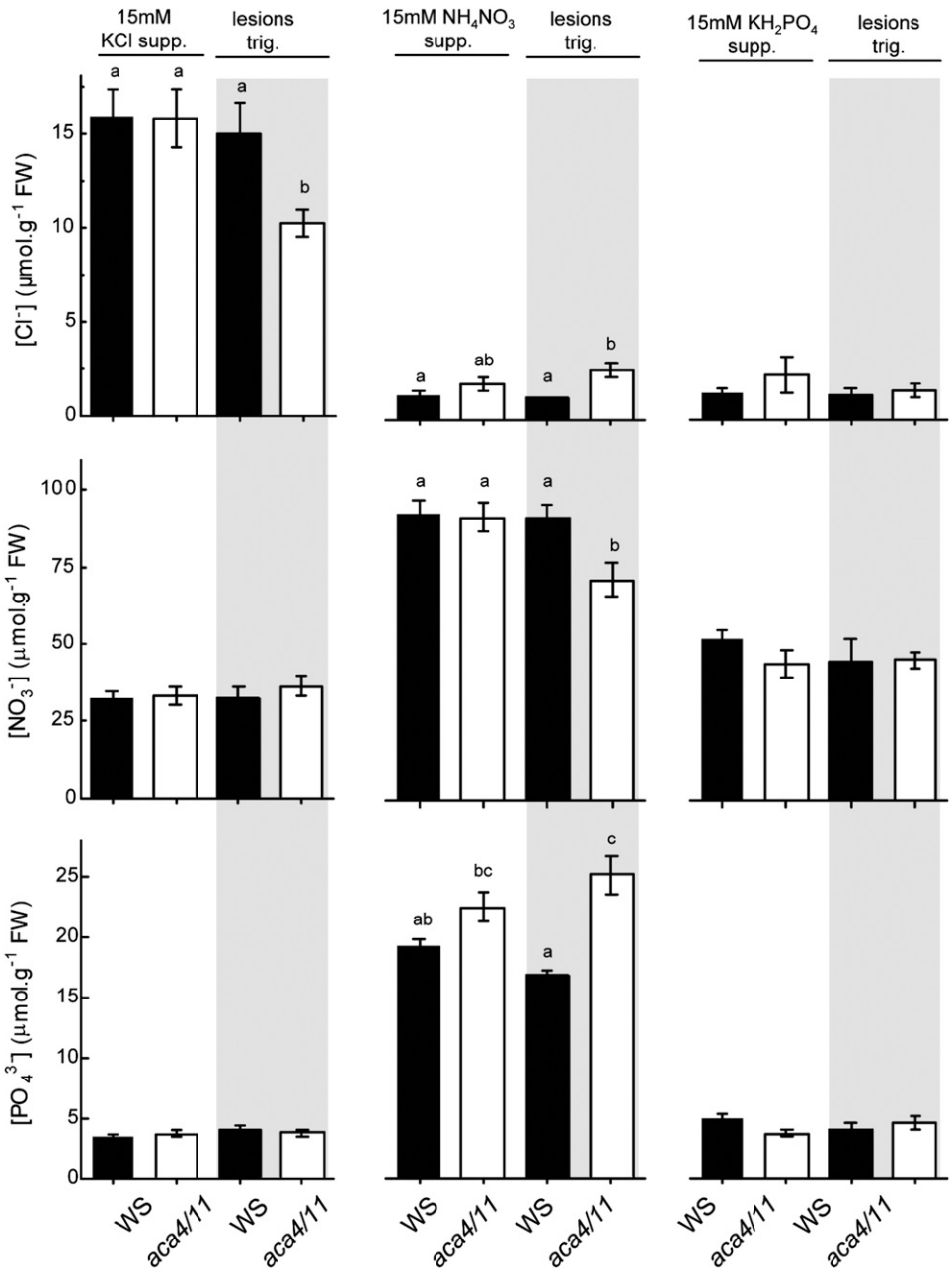

Figure 7. The *aca4/11* mutants show total anion levels similar to the wild type under lesion-suppressed conditions but a more rapid loss of Cl^- and NO_3^- when transferred to lesion induction conditions. Twenty-day-old plants were grown hydroponically under 15 mM KCl (left), 15 mM NH_4NO_3 (middle), or 15 mM KH_2PO_4 (right) before harvesting (white background; "supp.") or transferred into regular hydroponic solution 30 h prior to harvesting (gray background; "lesions trig."). Anion content was determined after chloroform/water extraction using liquid chromatography and normalized to the fresh weight (FW) of extracted leaves. Average results (±SE) for two independent experiments ($n > 16$ for KCl and NH_4NO_3 suppression experiments and $n = 6$ for KH_2PO_4 suppression experiments) are presented for Ws wild-type plants (black bars) and *aca4-1/11-1* plants (white bars). Within a subgraph, conditions sharing common labels (letters) are not significantly different from each other ($P > 0.05$).

In contrast to suppression by KCl and NH_4NO_3, suppression by 15 mM KH_2PO_4 was not accompanied by any detectable changes in free concentration of the corresponding anion (i.e. PO_4^{3-}; Fig. 7, right panels). However, it is important to note that our assay was limited to measuring the free concentration of PO_4^{3-} and did not account for other forms of phosphorus. Since free PO_4^{3-} levels are expected to be tightly regulated, any difference between the mutant and the wild type may have been masked by a rapid homeostasis mechanism that converts PO_4^{3-} to other forms, such as phytate (Loewus and Murthy, 2000).

Despite the inherent difficulty in accounting for the fate of free PO_4^{3-} during these suppression/induction experiments, the relatively rapid loss of NO_3^- and Cl^- in mutants upon moving plants to lesion-triggering conditions indicates that homeostasis controls for at least some anions are perturbed by the *aca4/11* mutations.

SA Signaling Is Activated in the *aca4/11* Mutant

In plants, SA can function as a signaling molecule to trigger defense responses, including a PCD pathway (Lorrain et al., 2003). To determine if the lesions associated with *aca4-1/11-1* involved an SA signal, we examined *aca4/11* mutants harboring a *sid2-5* mutation that disrupts SA biosynthesis (Nawrath and Métraux,

1999) as well as a *NahG* transgene that encodes an enzyme that increases the degradation rate of SA (Gaffney et al., 1993; Delaney et al., 1994). Both strategies resulted in the suppression of lesions (Fig. 8). This genetic suppression was observed in plants grown in soil or under standard hydroponic conditions.

To confirm that endogenous SA levels were up-regulated in *aca4/11* mutants, SA was measured in plants before and 30 h after moving hydroponically grown plants to lesion-inducing conditions. At both time points, mutants showed a 2-fold higher level of SA compared with the wild type (Supplemental Fig. S5). It is noteworthy that the SA levels were not significantly reduced when growing plants under suppressed conditions with high-anion supplements (Supplemental Fig. S5, 0 h). This suggests that the small 2-fold increase in SA by itself is not sufficient for lesion formation but requires other signaling functions that can somehow be suppressed by factors related to an increase in nutritional supplements.

Pathogen Defense Responses Occur More Quickly in *aca4/11* Mutants

Infection by the bacterial pathogen *Pseudomonas syringae* pv *tomato* DC3000 was used as a system to monitor a pathogen response in *aca4/11* plants. The response was evaluated by measuring bacterial growth (Fig. 9, A and B) as well as the expression of a defense-related marker gene, *PR1* (Fig. 9C; Uknes et al., 1992). These experiments were done under lesion suppression conditions to avoid having any pre-existing lesions that could potentially alter a pathogen attack.

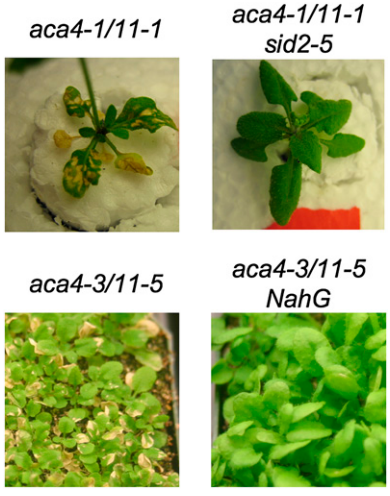

Figure 8. Lesions in *aca4/11* mutants can be suppressed by reducing the levels of SA. Photographs show *aca4-1/11-1* with and without a *sid2-5* mutation 10 d after transfer into hydroponic solution. A similar phenotype is observed with *NahG* expressed in *aca4-3/11-5*. See Figure 2, A and B, for comparison with *aca4/11* mutants.

Under lesion suppression conditions, the SA-inducible *PR1* gene showed no detectable expression in any of the plants lines tested (Fig. 9C, 0 h). Nevertheless, when lesion suppression conditions were removed and *aca4/11* mutants were allowed to develop their SA-dependent lesions, an up-regulation of the *PR1* marker gene was observed (data not shown).

Although our lesion suppression conditions prevented the formation of spontaneous SA-dependent lesions as well as the up-regulation of a SA-triggered pathogen defense marker gene (e.g. *PR1*), the actual defense response to a *P. syringae* pathogen attack was significantly faster and more effective in the *aca4/11* mutant, as indicated by lower bacterial growth at 2 and 3 d post inoculation (Fig. 9A) as well as by a more rapid induction of a *PR1* marker gene (by at least 12 h; Fig. 9C). This accelerated defense response was dependent upon SA, as shown using the *sid2-5* allele to block SA biosynthesis. By including the *sid2-5* mutation with *aca4-3* and *aca11-5* (Fig. 9B), the *aca4/11*-dependent inhibition of bacterial growth was reversed and the faster pathogen-triggered up-regulation of the *PR1* gene was abolished (Fig. 9C). A visual indication that *aca4/11* knockout accelerated the defense response was also confirmed by the more rapid development of HR lesions, which were clearly visible in the *aca4/11* mutant at 54 h post inoculation but not yet apparent in the wild-type control (Fig. 9D). These pathogen-triggered lesions were morphologically indistinguishable from the spontaneous lesions originally documented as the characteristic feature of the *aca4/11* lesion-mimic phenotype (Fig. 2).

DISCUSSION

Vacuolar Ca^{2+} Pumps Can Modulate the Initiation and Spread of HR-Like Lesions

Our analysis provides genetic evidence for a PCD pathway in plants whose initiation and cell-to-cell propagation can be suppressed by the activity of vacuolar Ca^{2+} pumps. This conclusion is based on the observation that two independent double *T-DNA* disruptions of vacuolar Ca^{2+} pumps *ACA4* and *ACA11* in Arabidopsis result in plants that begin developing lesions in rosette leaves early in development. Mutant plants, although smaller, can live for long periods of time and set seed. The lesion phenotype is weak or absent from single mutants, indicating that ACA4 and ACA11 provide some level of redundancy. While the Arabidopsis genome encodes 14 different Ca^{2+} pumps, a lesion phenotype has not yet been uncovered for any other combination of Ca^{2+} pump disruptions (McAinsh and Pittman, 2009; J.F. Harper, unpublished data). Thus, at present, the vacuolar Ca^{2+} pumps ACA4 and ACA11 define a specific Ca^{2+} efflux pathway that can function to suppress a PCD pathway in plants.

It is not yet clear if there is also a specific vacuolar Ca^{2+} influx channel involved in triggering the *aca4/11*-

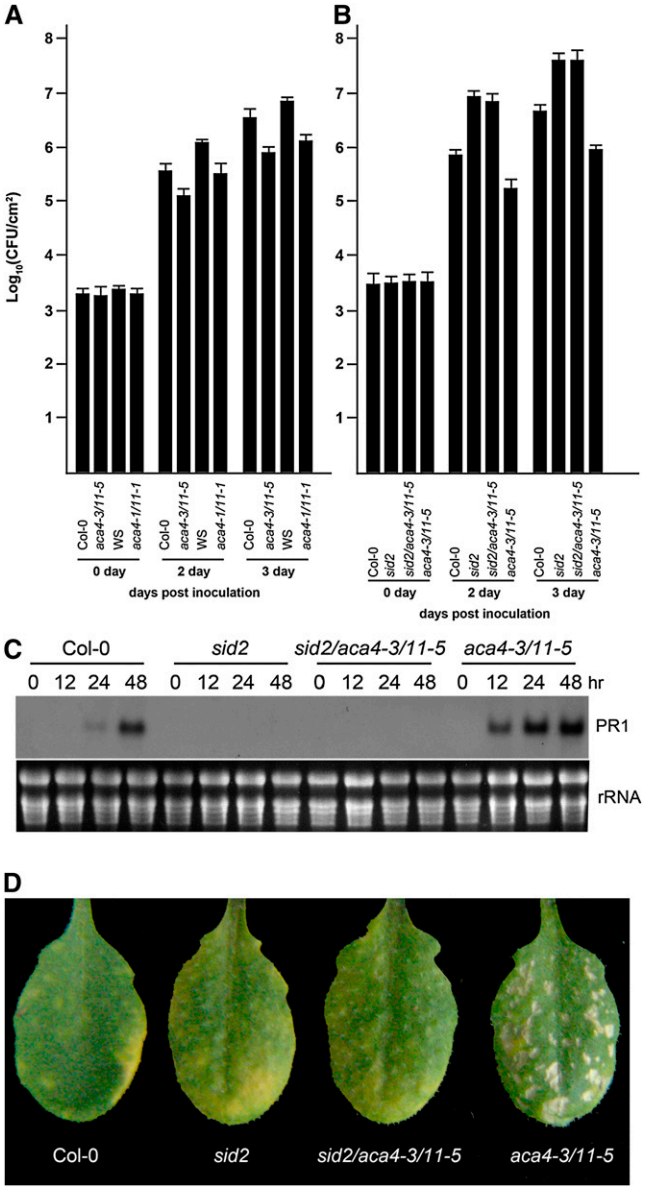

Figure 9. A SA-dependent pathogen defense response is accelerated by an *aca4/11* knockout. Leaves of 4-week-old plants (wild-type Col-0, *sid2*, *sid2/aca4/11*, and *aca4/11*) grown under lesion-suppressed conditions (50 mM KH_2PO_4) were sprayed with suspensions of *P. syringae* DC3000 (optical density at 600 nm = 0.01). A and B, Bacterial growth determinations were performed at the times indicated. Data points are averages of three replicate samples ± SD. CFU, Colony-forming units. C, Total RNA was isolated from leaves harvested at the indicated time points after bacterial inoculation. The section labeled PR1 shows an autoradiogram of a northern blot probed for the defense-related gene *PR1*. The section labeled rRNA shows a control for equal loading of RNA, as visualized by ethidium bromide staining of rRNAs. The northern blot shown is representative of two independent experiments showing equivalent results. D, Representative leaves from the different plant lines assayed are shown 54 h after bacterial inoculation. Note the fully developed lesions in the *aca4/11* leaf, whereas the other leaves show only yellow chlorotic patches.

PCD pathway. Evidence supporting a role for a TPC-type Ca^{2+} channel in a pathogen-induced HR response was previously reported for rice (*Oryza sativa*) and tobacco tissue culture cells (Kadota et al., 2004; Kurusu et al., 2005). However, these studies proposed a plasma membrane location for the TPC being analyzed. In contrast, evidence from Arabidopsis indicates that its single TPC homolog functions as part of the vacuole (Peiter et al., 2005; Ranf et al., 2008). In addition, a knockout of the Arabidopsis homolog (*tpc1-2*) failed to show an altered phenotype in response to elicitors or a fungal infection (Bonaventure et al., 2007; Ranf et al., 2008). Nevertheless, additional studies will be required to determine if the vacuolar TPC in Arabidopsis can function alone or in conjunction with other putative Ca^{2+} channels to trigger an *aca4/11*-dependent PCD pathway.

The *aca4/11* mutant can be classified as having a lesion-mimic phenotype, since the lesions have features consistent with a classical HR but can initiate in a sterile environment without a pathogen trigger (data not shown). Lesion-mimic mutants are often classified as either lesion-initiating or lesion-spreading mutants (Lorrain et al., 2003). The *aca4/11* mutation is unusual, since both initiation and spreading appear to be enhanced. When lesion suppression conditions were removed (Fig. 4), lesion initiation appeared to increase and macrolesions grew rapidly to cover most of the leaf surface within 1 week.

In plants and animals, three different cell death mechanisms have been described: (1) apoptosis-like PCD (AL-PCD); (2) autophagy-mediated PCD; and (3) nonprogrammed necrosis. Since HR lesions are considered to be a form of AL-PCD, the *aca4/11* lesions can also be classified as a form of AL-PCD. An easily visualized feature of HR lesions is an increase in callose synthesis at lesion initials. This requires a reprogramming of the cellular machinery and was observed as a feature of *aca4/11* lesions (Figs. 4 and 5). This supports the contention that *aca4/11* lesions develop as part of a PCD, as opposed to a spontaneous and rapid cellular necrosis.

Propagation of *aca4/11* Lesions Involves an SA-Dependent PCD Pathway

Two genetic lines of evidence indicate that *aca4/11*-dependent lesions propagate through a SA-dependent PCD pathway (Fig. 7; Supplemental Fig. S5). First, lesions were suppressed by a *sid2* mutation. The *sid2-5* mutation used here disrupts the isochorismate synthase gene *ICS1* (Wildermuth et al., 2001) and blocks the production of SA (Nawrath and Métraux, 1999). Second, lesions were suppressed by the expression of a *NahG* transgene. *NahG* encodes a bacterial salicylate hydroxylase that degrades SA into catechol (Gaffney et al., 1993; Delaney et al., 1994). This ability to block SA signaling and suppress *aca4/11* lesions confirms that lesion development results from a defect in regulating a specific PCD signal transduction pathway, as opposed to an uncontrolled cell death resulting from a

catastrophic defect in Ca^{2+} homeostasis or vacuolar degeneration.

Lesion Spread Can Be Suppressed by Anion Supplements

Interestingly, growth conditions were found that could separate lesion initiation from its uncontrolled spreading (Fig. 3). When mutant plants were grown with high concentrations of various anions, such as 15 to 20 mM NO_3^-, PO_4^-, or Cl^-, a high frequency of microlesions was still detected by staining leaves with aniline blue (Figs. 4 and 5; Supplemental Fig. S2). However, these lesions did not spread, indicating that the anion supplements functioned primarily to suppress a second distinct phase of lesion development (i.e. spreading). While the mechanism underlying anion suppression is not clear, suppression by NO_3^- and Cl^- did correlate with an increase in their concentrations in rosette leaves, followed by a more rapid loss compared with the wild type when transferred to unsupplemented growth conditions (Fig. 7). This supports a model in which the ionic environment at the site of lesion initiation and propagation can be altered to regulate a PCD pathway, potentially through changing ion conductance properties of either the plasma membrane or the vacuole.

Multiple studies have implicated nonspecific anion transporters in membrane depolarization events associated with many ion signaling pathways, including Ca^{2+} signals and PCD (Ward et al., 1995; Errakhi et al., 2008a, 2008b). For example, an anion efflux in tobacco leaf suspension cells was observed as an early response to the fungal elicitor cryptogein (Pugin et al., 1997). A pharmacological inhibition of this anion release was also observed to prevent the development of an HR in tobacco leaves (Wendehenne et al., 2002).

Using plants that were transferred from anion suppression to lesion-inducing conditions, the location of spontaneous lesion initials was found to be predominantly in mesophyll cells, without any correlation to being near to or far from vascular elements (Fig. 5; Supplemental Fig. S4). Since microlesions were never seen to appear in cell types of the root (i.e. no aniline blue-stained necrotic lesions), it is possible that lesion initiation and propagation are related to physiological triggers associated with photosynthetic pathways, as implicated in several examples of PCD triggered by abiotic stress (Gadjev et al., 2008).

It is noteworthy that ROS and SA levels in both anion-suppressed and nonsuppressed plants were approximately 2-fold higher than in controls (Fig. 4; Supplemental Fig. S5). Since the anion supplements did not block ROS and SA production but did prevent the accumulation of *PR1* (Fig. 9, 0 h), this suggests that the mechanism for anion suppression is at a point downstream of the initial signaling pathway that generates increased levels of SA or ROS and upstream of changes in the transcriptional response that upregulates *PR1* mRNA levels.

A Loss of *aca4* and *aca11* Potentiates an Accelerated Defense Response to *P. syringae*

An enhanced defense response against a bacterial pathogen, *P. syringae*, was observed here for *aca4/11* mutants (Fig. 9A). The defense response was tested under conditions in which spontaneous lesions in the *aca4/11* mutants were suppressed by anion supplements. The initial expression levels for an SA-up-regulated PR1 marker were undetectable in both mutants and wild-type controls under these conditions, although *aca4/11* mutants already showed a moderate elevation in SA (Supplemental Fig. S5). However, following a pathogen inoculation, the *aca4/11* mutants showed a more rapid induction of the *PR1* gene, with significant expression within 12 h (Fig. 9C). The enhanced resistance and more rapid induction of a *PR1* gene marker were both SA dependent, as indicated using a *sid2* mutation to block SA production (Fig. 9, B and C). These results suggest that even under lesion-suppressed conditions, the loss of *aca4/11* results in a physiologically altered plant that is preconditioned to a more rapid defense response and, therefore, confirm that ACA4 and ACA11 act as suppressors of a PCD pathway.

Evidence for Ca^{2+} Signals in Regulating PCD

Multiple lines of pharmacological and genetic evidence have implicated Ca^{2+} signals in regulating AL-PCD pathways in both animals (Clapham, 2007) and plants (Lecourieux et al., 2006; Ma and Berkowitz, 2007; Bosch and Franklin-Tong, 2008; Moeder and Yoshioka, 2008; Zhu et al., 2010). In plants, multiple proteins involved in Ca^{2+} signaling have been implicated in both positive and negative regulation of PCD. Recent examples include Ca^{2+}-binding copines (Liu et al., 2005; Lee and McNellis, 2009), the Ca^{2+}/calmodulin-interacting protein MLO in barley (*Hordeum vulgare*; Kim et al., 2002; Piffanelli et al., 2002), and the Ca^{2+}/calmodulin-binding transcription factor AtSR1 (Du et al., 2009). With respect to ion channels, a loss-of-function mutation in *CNGC2* (*dnd-1*) was found to have a lesion-suppressed phenotype (Clough et al., 2000). CNGCs in plants include isoforms that have features of being Ca^{2+}-permeable nonspecific ion channels that are gated open by cyclic nucleotides and feedback inhibited by Ca^{2+}/calmodulin (Talke et al., 2003; Frietsch et al., 2007; Ma and Berkowitz, 2007). Additionally, a gain-of-function CNGC mutation (*chimera of CNGC11 and CNGC12*) was identified with a lesion phenotype (Ma and Berkowitz, 2007; Urquhart et al., 2007; Moeder and Yoshioka, 2008). With respect to Ca^{2+} pumps, RNAi silencing of the tobacco *NbCA1* showed an acceleration of a pathogen-triggered PCD pathway (Zhu et al., 2010).

Evidence from both plant and animal examples provides strong support for the expectation that the activity of Ca^{2+} efflux pathways can modulate the magnitude and duration of Ca^{2+} signals in specific cellular

locations (Hetherington and Brownlee, 2004; Beauvois et al., 2006; Qudeimat et al., 2008; McAinsh and Pittman, 2009; Zhu et al., 2010). For example, in the moss *P. patens*, an engineered deletion of a vacuolar Ca^{2+} pump altered a salt stress-induced Ca^{2+} signal to be longer and of greater magnitude compared with the wild type (Qudeimat et al., 2008).

There are now several examples from plant and animal systems that implicate Ca^{2+} efflux systems as potential regulators of PCD. For example, an apoptosis phenotype was reported in animal smooth muscle cells in which the levels of two plasma membrane Ca^{2+} pumps had been reduced (Okunade et al., 2004; Prasad et al., 2007). In addition, apoptosis in animal cells has also been linked to a genetic disruption of Ca^{2+} pump activities in ER and Golgi locations (Okunade et al., 2007; Vafiadaki et al., 2009). In plants, the RNAi silencing of the Ca^{2+} pump *NbCA1* (Zhu et al., 2010) provides an example of an endomembrane Ca^{2+} pump that functions in modulating the kinetics of a pathogen-triggered PCD pathway.

The observation here that a loss of ACA4 and ACA11 increases the frequency of SA-dependent lesions is significant because it supports a new model in which the vacuole participates in modulating certain Ca^{2+} signals that can trigger PCD. Future research will be needed to visualize the Ca^{2+} signals that are altered by the loss of ACA4 and ACA11 and to understand the "upstream" factors that initiate those signals and the immediate "downstream" targets that link these signals to the activation of PCD. While it is known that Ca^{2+} efflux through ACAs can be turned on and off (Hwang et al., 2000), it remains to be determined if this activity is actually regulated as part of a natural mechanism by which a pathogen or abiotic stress might trigger the activation of a PCD pathway.

PCD is also involved in many other aspects of plant development, including senescence, sculpting of tissues, and the terminal differentiation of tracheids (Jones, 2001; Lam, 2004). While Ca^{2+} signals have been implicated in many of these pathways, it remains to be determined which pathways may involve Ca^{2+} signals modulated by vacuoles. Nevertheless, from a genetic perspective, this study identifies one function of the vacuolar pumps *ACA4* and *ACA11* as a suppressor of an SA-dependent PCD pathway. This function also represents a plant-specific variation on the regulation of PCD, since the large central vacuole in plant cells is a feature not found in typical animal cells.

MATERIALS AND METHODS

Plant Growth Conditions

Arabidopsis (*Arabidopsis thaliana*) seeds were surface sterilized for 3 h with chlorine gas (Clough and Bent, 1998) and then sown on plates on half-strength Murashige and Skoog medium complemented by 2% Suc and 10 g L^{-1} agar. After 2 d of vernalization in the dark at 4°C, seeds were germinated under continuous light at approximately 19°C. Nine-day-old seedlings were transferred to soil or hydroponics. Unless otherwise stated, plants in growth chambers were grown at 65% relative humidity, 16 h of light at 21°C, and 8 h of dark at 19°C. Greenhouse-grown plants were subject to seasonal variations in light and humidity. Soil used was Special Blend from Sunshine (Sun Gro). For hydroponic cultures, seedlings were transferred onto a floating foam support in a 3-L bucket filled with a standard hydroponic solution of 1.25 mM KNO_3, 0.75 mM $MgSO_4$, 1.5 mM $Ca(NO_3)_2$, 0.5 mM KH_2PO_4, 50 μM FeEDTA, 50 μM H_3BO_3, 12 μM $MnSO_4$, 0.7 μM $CuSO_4$, 1 μM $ZnSO_4$, 0.24 μM MoO_4Na_2, and 100 μM Na_2SiO_3. Hydroponic solutions were replaced weekly. For suppression conditions, the standard hydroponic solution above was supplemented as stated in the text.

Plant Material and Genotyping

Plants were transformed using *Agrobacterium tumefaciens* (GV3101 line) and a floral dip method (Clough and Bent, 1998). Dry seeds were harvested, and hygromycin-resistant plants (T1) were identified and grown for seeds. Plant genotypes were determined by PCR. Leaves of approximately 0.5 cm^2 were harvested and manually ground in an extraction buffer (250 mM NaCl, 200 mM Tris, pH 8.0, 25 mM EDTA, and 0.1% SDS), and debris was pelleted by a 10-min centrifugation at 10,000*g*. DNA in the supernatant was recovered by 66% ispopropanol precipitation. Touchdown PCR (from 66°C to 60°C in −0.3°C steps, and then 14 additional cycles with an annealing temperature of 60°C) was performed in a 25-μL reaction using ExTaq DNA polymerase (Takara) following the manufacturer's protocol. Oligonucleotides used for the reaction, at a final concentration of 0.2 μM, are listed in the legend of Figure 1.

Inoculation of Plants with *Pseudomonas syringae*

The virulent *Pseudomonas syringae* pv *tomato* DC3000 was grown at 28°C on King B's medium (40 g L^{-1} Proteose Peptone 3, 20 g L^{-1} glycerin, 10 mL L^{-1} $MgSO_4$ [10% m/v], and 10 mL L^{-1} K_2HPO_4 [10% m/v]) supplemented with the appropriate antibiotics: 50 mg mL^{-1} rifampicin. To examine the growth of the bacteria, 3- to 4-week-old plants were sprayed with a bacterial suspension containing 5×10^6 colony-forming units per mL in 10 mM $MgCl_2$ solution with 0.04% Silwet L-77. Bacterial growth was measured at 0, 2, and 3 d after infiltration by extracting bacteria from leaf discs (0.6 cm^2 discs per leaf) and plating a series of dilutions on the medium supplemented with appropriate antibiotics.

Plasmid Constructs

Plant expression constructs were made in the pGreenII vector system (Hellens et al., 2000) with a kanamycin selection marker for bacteria and a hygromycin marker for plants. The *35S::ACA11-GFP* (ps#1658) construct was described previously (Lee et al., 2007). For the *ACA11p::ACA11-GFP* construct (ps#1657), a 2,127-bp sequence upstream of the *ATG* start codon for *ACA11* was PCR amplified from Arabidopsis and replaced the *35S* promoter of *35S-ACA11-GFP* (ps#1658). The DNA sequence of each construct is provided in Supplemental Figure S6.

Northern-Blot Analysis

Total RNA was isolated from leaves using the LiCl-phenol/chloroform extraction method (Chomczynski and Sacchi, 2006). Total RNA (10 μg) was separated on 1.5% agarose-formaldehyde gels and blotted onto nylon membranes. The membranes were hybridized with [α-^{32}P]dATP-labeled gene-specific probes for 16 h at 65°C and washed for 10 min twice with 2× SSC (0.15 M NaCl and 15 mM trisodium citrate), once with 1× SSC, and for 10 min with 0.5× SSC and 1% (w/v) SDS at 65°C.

Western-Blot Analysis

Membrane proteins (30 μg) were isolated from ACA11-GFP transgenic mutant plants and separated by 8% SDS-PAGE. A rabbit anti-GFP antibody (Santa Cruz Biotechnology) was used to probe a western blot and visualized using a goat anti-rabbit IgG antibody (Calbiochem) and Enhanced Chemical Luminescence detection according to the manufacturer's protocol (GE Healthcare).

Detection of ROS and Callose

Excised leaves were vacuum infiltrated with a solution of 1 mg mL^{-1} 3,3′-diaminobenzidine (Sigma) and then stored for 3 h on wet paper under lights.

Leaves were then fixed and bleached overnight with a solution of ethanol: lactic acid:glycerol (3:1:1 in volume), washed with decreasing ethanol concentrations (75%, 50%, 25%), and equilibrated in water. Photographs were taken with a digital camera using a dissecting microscope. Diaminobenzidine staining appeared as a brown deposit.

Detection of callose in leaves was performed essentially as described (Dietrich et al., 1994). The two largest leaves were fixed for 2 h in 10% formaldehyde, 5% acetic acid, and 45% ethanol, cleared for 2 min in boiling alcoholic lactophenol (95% ethanol:lactophenol, 2:1), and stained overnight in a solution of 150 mM K_2HPO_4, pH 9.5, with 0.01% aniline blue. Leaves were rinsed in distilled water before observation. Callose deposition was observed with an Olympus FV1000 confocal microscope with 405-nm excitation and a 440- to 480-nm emission window. Six Z-sections (640 μm $\times$ 640 μm) spanning the whole leaf thickness were taken per leaf. Lesion surface and number were obtained from an analysis of every section in the stack.

Ion Concentration Measurements

Four- to 5-week old rosette leaves were harvested, and their dry weight was determined after incubation for 3 d at 110°C. Dried tissue was digested overnight with 3 mL of concentrated HNO_3, and cation content was determined using ICP-AES (Varian). To determine the concentrations of anions, 4- to 5-week-old rosette leaves were harvested, weighed, and processed by one of two procedures. Samples were either ground in liquid nitrogen and resuspended in 3 mL of chloroform, or frozen samples were ground directly in 3 mL of HPLC-grade chloroform using a mixer mill (Retsch). Samples were then incubated in 15-mL polypropylene tubes for 1 h at 50°C. Ultrapure water (5 mL) was added, and samples were incubated for an additional 1 h. Tubes were centrifuged for 15 min at 2,900*g* to clear debris from the aqueous phase. The supernatant was analyzed by anion-exchange chromatography. Aliquots of the supernatant (10 μL) were run on a Dionex HPLC apparatus through a Dionex AS11-HC column with a gradient of 1 to 60 mM NaOH over 40 min. The column was at room temperature with a flow rate of 0.27 mL min^{-1}. Anions were detected by the suppressed conductivity method, and NO_3^- was specifically detected by A_{210}. Peaks were identified using pure anion salt standards purchased from Sigma.

Supplemental Data

The following materials are available in the online version of this article.

Supplemental Figure S1. Images of *aca4-1/11-1* leaves showing increased ROS accumulation and callose deposits, as revealed by diaminobenzidine or aniline blue staining.

Supplemental Figure S2. Representative images showing lesion initials in mesophyll cells in *aca4-1/11-1* plants.

Supplemental Figure S3. Frequency of lesion initials with respect to vessels.

Supplemental Figure S4. Ion concentrations of eight mineral nutrients in leaves from *aca4-1/11-1* and Ws plants.

Supplemental Figure S5. Relative SA levels in *aca4-1/11-1* upon lesion induction.

Supplemental Figure S6. DNA sequence of the *ACA11-GFP* plasmid constructs used for mutant rescues.

ACKNOWLEDGMENTS

We thank Dave Quillici for his help in mass spectrometry, Meral Tunc for discussions and technical assistance, and Saskia van Wees and Jane Glazebrook for *sid2-5* and *NahG* plant lines.

Received May 11, 2010; accepted September 9, 2010; published September 13, 2010.

LITERATURE CITED

Alonso JM, Stepanova AN, Leisse TJ, Kim CJ, Chen H, Shinn P, Stevenson DK, Zimmerman J, Barajas P, Cheuk R, et al (2003) Genome-wide insertional mutagenesis of Arabidopsis thaliana. Science **301:** 653–657

Baxter I, Tchieu J, Sussman MR, Boutry M, Palmgren MG, Gribskov M, Harper JF, Axelsen KB (2003) Genomic comparison of P-type ATPase ion pumps in Arabidopsis and rice. Plant Physiol **132:** 618–628

Beauvois MC, Merezak C, Jonas JC, Ravier MA, Henquin JC, Gilon P (2006) Glucose-induced mixed [Ca^{2+}]c oscillations in mouse beta-cells are controlled by the membrane potential and the SERCA3 Ca^{2+}-ATPase of the endoplasmic reticulum. Am J Physiol Cell Physiol **290:** C1503–C1511

Bonaventure G, Gfeller A, Rodríguez VM, Armand F, Farmer EE (2007) The fou2 gain-of-function allele and the wild-type allele of Two Pore Channel 1 contribute to different extents or by different mechanisms to defense gene expression in Arabidopsis. Plant Cell Physiol **48:** 1775–1789

Bosch M, Franklin-Tong VE (2008) Self-incompatibility in Papaver: signalling to trigger PCD in incompatible pollen. J Exp Bot **59:** 481–490

Bothwell JHF, Kisielewska J, Genner MJ, McAinsh MR, Brownlee C (2008) Ca^{2+} signals coordinate zygotic polarization and cell cycle progression in the brown alga Fucus serratus. Development **135:** 2173–2181

Boursiac Y, Harper JF (2007) The origin and function of calmodulin regulated Ca^{2+} pumps in plants. J Bioenerg Biomembr **39:** 409–414

Chomczynski P, Sacchi N (2006) The single-step method of RNA isolation by acid guanidinium thiocyanate-phenol-chloroform extraction: twenty-something years on. Nat Protoc **1:** 581–585

Clapham DE (2007) Calcium signaling. Cell **131:** 1047–1058

Clough SJ, Bent AF (1998) Floral dip: a simplified method for Agrobacterium-mediated transformation of Arabidopsis thaliana. Plant J **16:** 735–743

Clough SJ, Fengler KA, Yu IC, Lippok B, Smith RK Jr, Bent AF (2000) The Arabidopsis dnd1 "defense, no death" gene encodes a mutated cyclic nucleotide-gated ion channel. Proc Natl Acad Sci USA **97:** 9323–9328

Delaney TP, Uknes S, Vernooij B, Friedrich L, Weymann K, Negrotto D, Gaffney T, Gut-Rella M, Kessmann H, Ward E, et al (1994) A central role of salicylic acid in plant disease resistance. Science **266:** 1247–1250

Dietrich RA, Delaney TP, Uknes SJ, Ward ER, Ryals JA, Dangl JL (1994) Arabidopsis mutants simulating disease resistance response. Cell **77:** 565–577

Dodd AN, Kudla J, Sanders D (2010) The language of calcium signaling. Annu Rev Plant Biol **61:** 593–620

Du L, Ali GS, Simons KA, Hou J, Yang T, Reddy ASN, Poovaiah BW (2009) Ca(2+)/calmodulin regulates salicylic-acid-mediated plant immunity. Nature **457:** 1154–1158

Errakhi R, Dauphin A, Meimoun P, Lehner A, Reboutier D, Vatsa P, Briand J, Madiona K, Rona JP, Barakate M, et al (2008a) An early Ca^{2+} influx is a prerequisite to thaxtomin A-induced cell death in Arabidopsis thaliana cells. J Exp Bot **59:** 4259–4270

Errakhi R, Meimoun P, Lehner A, Vidal G, Briand J, Corbineau F, Rona JP, Bouteau F (2008b) Anion channel activity is necessary to induce ethylene synthesis and programmed cell death in response to oxalic acid. J Exp Bot **59:** 3121–3129

Frietsch S, Wang YF, Sladek C, Poulsen LR, Romanowsky SM, Schroeder JI, Harper JF (2007) A cyclic nucleotide-gated channel is essential for polarized tip growth of pollen. Proc Natl Acad Sci USA **104:** 14531–14536

Gadjev I, Stone JM, Gechev TS (2008) Programmed cell death in plants: new insights into redox regulation and the role of hydrogen peroxide. Int Rev Cell Mol Biol **270:** 87–144

Gaffney T, Friedrich L, Vernooij B, Negrotto D, Nye G, Uknes S, Ward E, Kessmann H, Ryals J (1993) Requirement of salicylic acid for the induction of systemic acquired resistance. Science **261:** 754–756

Geisler M, Frangne N, Gomès E, Martinoia E, Palmgren MG (2000) The ACA4 gene of Arabidopsis encodes a vacuolar membrane calcium pump that improves salt tolerance in yeast. Plant Physiol **124:** 1814–1827

George L, Romanowsky SM, Harper JF, Sharrock RA (2008) The ACA10 Ca^{2+}-ATPase regulates adult vegetative development and inflorescence architecture in Arabidopsis. Plant Physiol **146:** 716–728

Hellens RP, Edwards EA, Leyland NR, Bean S, Mullineaux PM (2000) pGreen: a versatile and flexible binary Ti vector for Agrobacterium-mediated plant transformation. Plant Mol Biol **42:** 819–832

Hetherington AM, Brownlee C (2004) The generation of Ca(2+) signals in plants. Annu Rev Plant Biol **55:** 401–427

Hirschi KD (1999) Expression of *Arabidopsis* CAX1 in tobacco: altered calcium homeostasis and increased stress sensitivity. Plant Cell **11:** 2113–2122

Hwang I, Sze H, Harper JF (2000) A calcium-dependent protein kinase can inhibit a calmodulin-stimulated Ca^{2+} pump (ACA2) located in the endoplasmic reticulum of Arabidopsis. Proc Natl Acad Sci USA **97:** 6224–6229

Israelsson M, Siegel RS, Young J, Hashimoto M, Iba K, Schroeder JI (2006) Guard cell ABA and CO_2 signaling network updates and Ca^{2+} sensor priming hypothesis. Curr Opin Plant Biol **9:** 654–663

Jones AM (2001) Programmed cell death in development and defense. Plant Physiol **125:** 94–97

Kadota Y, Furuichi T, Ogasawara Y, Goh T, Higashi K, Muto S, Kuchitsu K (2004) Identification of putative voltage-dependent Ca^{2+}-permeable channels involved in cryptogein-induced Ca^{2+} transients and defense responses in tobacco BY-2 cells. Biochem Biophys Res Commun **317:** 823–830

Kim CK, Han JS, Lee HS, Oh JY, Shigaki T, Park SH, Hirschi K (2006) Expression of an Arabidopsis CAX2 variant in potato tubers increases calcium levels with no accumulation of manganese. Plant Cell Rep **25:** 1226–1232

Kim MC, Panstruga R, Elliott C, Müller J, Devoto A, Yoon HW, Park HC, Cho MJ, Schulze-Lefert P (2002) Calmodulin interacts with MLO protein to regulate defence against mildew in barley. Nature **416:** 447–451

Kosuta S, Hazledine S, Sun J, Miwa H, Morris RJ, Downie JA, Oldroyd GED (2008) Differential and chaotic calcium signatures in the symbiosis signaling pathway of legumes. Proc Natl Acad Sci USA **105:** 9823–9828

Kudla J, Batistic O, Hashimoto K (2010) Calcium signals: the lead currency of plant information processing. Plant Cell **22:** 541–563

Kurusu T, Yagala T, Miyao A, Hirochika H, Kuchitsu K (2005) Identification of a putative voltage-gated Ca^{2+} channel as a key regulator of elicitor-induced hypersensitive cell death and mitogen-activated protein kinase activation in rice. Plant J **42:** 798–809

Lam E (2004) Controlled cell death, plant survival and development. Nat Rev Mol Cell Biol **5:** 305–315

Lecourieux D, Ranjeva R, Pugin A (2006) Calcium in plant defence-signalling pathways. New Phytol **171:** 249–269

Lee SM, Kim HS, Han HJ, Moon BC, Kim CY, Harper JF, Chung WS (2007) Identification of a calmodulin-regulated autoinhibited Ca^{2+}-ATPase (ACA11) that is localized to vacuole membranes in Arabidopsis. FEBS Lett **581:** 3943–3949

Lee TF, McNellis TW (2009) Evidence that the BONZAI1/COPINE1 protein is a calcium- and pathogen-responsive defense suppressor. Plant Mol Biol **69:** 155–166

Li X, Chanroj S, Wu Z, Romanowsky SM, Harper JF, Sze H (2008) A distinct endosomal Ca^{2+}/Mn^{2+} pump affects root growth through the secretory process. Plant Physiol **147:** 1675–1689

Liu J, Jambunathan N, McNellis TW (2005) Transgenic expression of the von Willebrand A domain of the BONZAI 1/COPINE 1 protein triggers a lesion-mimic phenotype in Arabidopsis. Planta **221:** 85–94

Loewus FA, Murthy PPN (2000) Myo-inositol metabolism in plants. Plant Sci **150:** 1–19

Lorrain S, Lin B, Auriac MC, Kroj T, Saindrenan P, Nicole M, Balagué C, Roby D (2004) Vascular associated death1, a novel GRAM domain-containing protein, is a regulator of cell death and defense responses in vascular tissues. Plant Cell **16:** 2217–2232

Lorrain S, Vailleau F, Balagué C, Roby D (2003) Lesion mimic mutants: keys for deciphering cell death and defense pathways in plants? Trends Plant Sci **8:** 263–271

Ma W, Berkowitz GA (2007) The grateful dead: calcium and cell death in plant innate immunity. Cell Microbiol **9:** 2571–2585

Ma W, Smigel A, Tsai YC, Braam J, Berkowitz GA (2008) Innate immunity signaling: cytosolic Ca^{2+} elevation is linked to downstream nitric oxide generation through the action of calmodulin or a calmodulin-like protein. Plant Physiol **148:** 818–828

Mahajan S, Pandey GK, Tuteja N (2008) Calcium- and salt-stress signaling in plants: shedding light on SOS pathway. Arch Biochem Biophys **471:** 146–158

McAinsh MR, Pittman JK (2009) Shaping the calcium signature. New Phytol **181:** 275–294

McElver J, Tzafrir I, Aux G, Rogers R, Ashby C, Smith K, Thomas C, Schetter A, Zhou Q, Cushman MA, et al (2001) Insertional mutagenesis of genes required for seed development in Arabidopsis thaliana. Genetics **159:** 1751–1763

Moeder W, Yoshioka K (2008) Lesion mimic mutants: a classical, yet still fundamental approach to study programmed cell death. Plant Signal Behav **3:** 764–767

Nawrath C, Métraux JP (1999) Salicylic acid induction-deficient mutants of *Arabidopsis* express PR-2 and PR-5 and accumulate high levels of camalexin after pathogen inoculation. Plant Cell **11:** 1393–1404

Neill S, Barros R, Bright J, Desikan R, Hancock J, Harrison J, Morris P, Ribeiro D, Wilson I (2008) Nitric oxide, stomatal closure, and abiotic stress. J Exp Bot **59:** 165–176

Okunade GW, Miller ML, Azhar M, Andringa A, Sanford LP, Doetschman T, Prasad V, Shull GE (2007) Loss of the Atp2c1 secretory pathway Ca(2+)-ATPase (SPCA1) in mice causes Golgi stress, apoptosis, and midgestational death in homozygous embryos and squamous cell tumors in adult heterozygotes. J Biol Chem **282:** 26517–26527

Okunade GW, Miller ML, Pyne GJ, Sutliff RL, O'Connor KT, Neumann JC, Andringa A, Miller DA, Prasad V, Doetschman T, et al (2004) Targeted ablation of plasma membrane Ca^{2+}-ATPase (PMCA) 1 and 4 indicates a major housekeeping function for PMCA1 and a critical role in hyperactivated sperm motility and male fertility for PMCA4. J Biol Chem **279:** 33742–33750

Oldroyd GED, Downie JA (2004) Calcium, kinases and nodulation signalling in legumes. Nat Rev Mol Cell Biol **5:** 566–576

Pandey S, Zhang W, Assmann SM (2007) Roles of ion channels and transporters in guard cell signal transduction. FEBS Lett **581:** 2325–2336

Peiter E, Maathuis FJM, Mills LN, Knight H, Pelloux J, Hetherington AM, Sanders D (2005) The vacuolar Ca^{2+}-activated channel TPC1 regulates germination and stomatal movement. Nature **434:** 404–408

Piffanelli P, Zhou F, Casais C, Orme J, Jarosch B, Schaffrath U, Collins NC, Panstruga R, Schulze-Lefert P (2002) The barley MLO modulator of defense and cell death is responsive to biotic and abiotic stress stimuli. Plant Physiol **129:** 1076–1085

Pottosin II, Schönknecht G (2007) Vacuolar calcium channels. J Exp Bot **58:** 1559–1569

Prasad V, Okunade G, Liu L, Paul RJ, Shull GE (2007) Distinct phenotypes among plasma membrane Ca^{2+}-ATPase knockout mice. Ann N Y Acad Sci **1099:** 276–286

Pugin A, Frachisse JM, Tavernier E, Bligny R, Gout E, Douce R, Guern J (1997) Early events induced by the elicitor cryptogein in tobacco cells: involvement of a plasma membrane NADPH oxidase and activation of glycolysis and the pentose phosphate pathway. Plant Cell **9:** 2077–2091

Qudeimat E, Faltusz AMC, Wheeler G, Lang D, Brownlee C, Reski R, Frank W (2008) A PIIB-type Ca^{2+}-ATPase is essential for stress adaptation in Physcomitrella patens. Proc Natl Acad Sci USA **105:** 19555–19560

Ranf S, Wünnenberg P, Lee J, Becker D, Dunkel M, Hedrich R, Scheel D, Dietrich P (2008) Loss of the vacuolar cation channel, AtTPC1, does not impair Ca^{2+} signals induced by abiotic and biotic stresses. Plant J **53:** 287–299

Reape TJ, Molony EM, McCabe PF (2008) Programmed cell death in plants: distinguishing between different modes. J Exp Bot **59:** 435–444

Schiøtt M, Romanowsky SM, Baekgaard L, Jakobsen MK, Palmgren MG, Harper JF (2004) A plant plasma membrane Ca^{2+} pump is required for normal pollen tube growth and fertilization. Proc Natl Acad Sci USA **101:** 9502–9507

Sirichandra C, Wasilewska A, Vlad F, Valon C, Leung J (2009) The guard cell as a single-cell model towards understanding drought tolerance and abscisic acid action. J Exp Bot **60:** 1439–1463

Song WY, Zhang ZB, Shao HB, Guo XL, Cao HX, Zhao HB, Fu ZY, Hu XJ (2008) Relationship between calcium decoding elements and plant abiotic-stress resistance. Int J Biol Sci **4:** 116–125

Sussman MR, Amasino RM, Young JC, Krysan PJ, Austin-Phillips S (2000) The Arabidopsis knockout facility at the University of Wisconsin-Madison. Plant Physiol **124:** 1465–1467

Talke IN, Blaudez D, Maathuis FJM, Sanders D (2003) CNGCs: prime targets of plant cyclic nucleotide signalling? Trends Plant Sci **8:** 286–293

Uknes S, Mauch-Mani B, Moyer M, Potter S, Williams S, Dincher S, Chandler D, Slusarenko A, Ward E, Ryals J (1992) Acquired resistance in *Arabidopsis*. Plant Cell **4:** 645–656

Urquhart W, Gunawardena AHLAN, Moeder W, Ali R, Berkowitz GA, Yoshioka K (2007) The chimeric cyclic nucleotide-gated ion channel ATCNGC11/12 constitutively induces programmed cell death in a Ca^{2+} dependent manner. Plant Mol Biol **65:** 747–761

Vafiadaki E, Papalouka V, Arvanitis DA, Kranias EG, Sanoudou D (2009) The role of SERCA2a/PLN complex, Ca(2+) homeostasis, and anti-apoptotic proteins in determining cell fate. Pflugers Arch **457:** 687–700

Verkhratsky A (2007) Calcium and cell death. Subcell Biochem **45:** 465–480

Ward JM, Mäser P, Schroeder JI (2009) Plant ion channels: gene families, physiology, and functional genomics analyses. Annu Rev Physiol **71:** 59–82

Ward JM, Pei ZM, Schroeder JI (1995) Roles of ion channels in initiation of signal transduction in higher plants. Plant Cell **7:** 833–844

Wendehenne D, Lamotte O, Frachisse JM, Barbier-Brygoo H, Pugin A (2002) Nitrate efflux is an essential component of the cryptogein signaling pathway leading to defense responses and hypersensitive cell death in tobacco. Plant Cell **14:** 1937–1951

Wildermuth MC, Dewdney J, Wu G, Ausubel FM (2001) Isochorismate synthase is required to synthesize salicylic acid for plant defence. Nature **414:** 562–565

Wu Z, Liang F, Hong B, Young JC, Sussman MR, Harper JF, Sze H (2002) An endoplasmic reticulum-bound Ca^{2+}/Mn^{2+} pump, ECA1, supports plant growth and confers tolerance to Mn^{2+} stress. Plant Physiol **130:** 128–137

Zhu X, Caplan J, Mamillapalli P, Czymmek K, Dinesh-Kumar SP (2010) Function of endoplasmic reticulum calcium ATPase in innate immunity-mediated programmed cell death. EMBO J **29:** 1007–1018